

PSFC/RR-02-8

## Performance of a Compact Four-Strap Fast Wave Antenna



[Metadata, citation and similar papers at core.ac.u](#)

Provided by DSpace@MIT

Y. Lin, M. Porkolab, I.H. Hutchinson, E. Marmor,  
G. Schilling<sup>3</sup>, J.R. Wilson<sup>3</sup>

October 2002

Plasma Science and Fusion Center  
Massachusetts Institute of Technology  
Cambridge, MA 02139 USA

<sup>1</sup>Present address General Atomics, San Diego, CA 92186-5608 USA

<sup>2</sup>present address University of Wisconsin, Madison, WI 53706 USA

<sup>3</sup>Princeton Plasma Physics Laboratory, Princeton, NJ USA

This work was supported by the U.S. Department of Energy, Cooperative Grant No. DE-FC02-99ER54512. Reproduction, translation, publication, use and disposal, in whole or in part, by or for the United States government is permitted.

## Performance of a Compact Four-Strap Fast Wave Antenna

S.J. Wukitch,<sup>1</sup> R.L. Boivin,<sup>2</sup> P.T. Bonoli,<sup>1</sup> J.A. Goetz,<sup>3</sup> J. Hosea,<sup>4</sup> Y. Lin,<sup>1</sup> M. Porkolab,<sup>1</sup> I.H. Hutchinson,<sup>1</sup> E. Marmor,<sup>1</sup> G. Schilling,<sup>4</sup> and J.R. Wilson<sup>4</sup>

<sup>1</sup>MIT Plasma Science and Fusion Center, Cambridge MA 02139 USA

Email: [wukitch@psfc.mit.edu](mailto:wukitch@psfc.mit.edu)

<sup>2</sup>present address: General Atomics, P.O. Box 85608, San Diego CA 92186-5608 USA

<sup>3</sup>present address: University of Wisconsin, Madison WI 53706 USA

<sup>4</sup>Princeton Plasma Physics Laboratory, Princeton NJ USA

**Abstract.** Compact antennas with high power density able to withstand large disruption forces present significant challenges to ICRF antenna design. A compact four-strap antenna has been developed and installed in Alcator C-Mod. Here we describe the key design features of the antenna and assess its performance by comparison with a pair of two-strap antennas. The key design features are the long vacuum strip line feeds, folded current strap configuration, use of ceramic insulators in the Faraday screen, and open Faraday screen. The heating efficiency and impurity generation are nearly identical to the other antennas while the loading is  $\sim 2.5$  higher. To reach high power density operation, arcing and impurity generation problems, at relatively low maximum voltage, required some modifications. Inspection of the strip line and antenna strap showed arc damage localized to regions where the RF E-field was parallel to the tokamak B-field. For E||B, the breakdown voltage was determined to be  $\sim 15$  kV/cm. Redesign of the strip line to orient the RF E-field across the B-field resulted in an increase in the maximum voltage from 17 kV to 25 kV. To improve the maximum voltage further, the current strap was modified to decrease the E-field parallel to the tokamak B-field in the current strap itself. These modifications allowed the maximum injected power to reach  $\sim 3$  MW and  $\sim 35$  kV.

### 1.0 Introduction

Ion cyclotron range of frequency (ICRF) is expected to be a primary auxiliary heating source in future experiments and fusion reactors. High power density, compact antennas present significant challenges to ICRF antenna design. A compact 4-strap, fast-wave (J-port) antenna has been developed and installed in Alcator C-Mod in collaboration with Princeton Plasma Physics Laboratory (PPPL). The design challenge was to reliably deliver 3 MW (4 MW source) through a single horizontal port (63 cm x 20 cm), have a peak operational voltage of 40 kV, heat efficiently and allow for flexible phasing. Limited access dictated using a folded strap design and vacuum strip line for the antenna feeds. In addition, the Faraday screen and antenna box are more open than the original two 2-strap (D and E-port) antennas[1] to allow for a better current drive spectrum.

Antenna designs are often based upon the available experimental experience and theoretical models. Furthermore, antenna performance appears to be difficult to predict with the available simulation tools. For example, the ICRF antennas in the Joint European Torus (JET) have evolved from 2-strap antennas that coupled 22 MW of ICRF power to the plasma [2] to 4-strap antennas that couple 16 MW of ICRF power to the plasma.[3] In C-Mod, the 2-strap antennas have obtained power densities of  $\sim 10$  MW/m<sup>2</sup> and the original J-port antenna was limited to 5 MW/m<sup>2</sup>. [4] In general, the antenna performance can be limited by arcing or impurity generation and both these phenomena are inadequately understood. In the development of the J-port antenna, an empirical approach was adopted to overcome performance limitations due to arcing and impurity generation. Presented in the following is a brief description of the antennas and their key design features. This is followed by a discussion of the performance and comparison of the antennas.

## 2.0 Antenna Description

The C-Mod ICRF antennas are required to be compact, withstand high heat loads and large disruption forces, and hold off RF high voltages in presence of 0.1-1 mTorr neutral pressures. The two 2-strap, fast wave antennas, D and E-port antennas, have delivered 3.5 MW through two horizontal ports and have a fixed dipole phase.[1] This corresponds to a power density of  $\sim 10 \text{ MW/m}^2$ . The J-port antenna was designed to utilize a single horizontal port resulting in expected power density of  $11 \text{ MW/m}^2$  at 3 MW coupled power.

The D and E-port antennas (D-port is shown in FIG.1) have end-fed center grounded current straps and the vacuum transmission line is  $30 \Omega$  strip line. The protection tiles are boron nitride (BN). The Faraday screen is aligned with the nominal magnetic field pitch,  $\sim 10^\circ$  and is  $\sim 27\%$  optically transparent. The screen elements are 0.95 cm diameter, Cu-plated, (4-8  $\mu\text{m}$ ) Inconel 625 rods welded to the antenna box at both ends. The Faraday rods are coated with TiCN on D-port and  $\text{B}_4\text{C}$  on E-port. Due to the large disruption forces generated by  $\sim 1 \text{ T/msec}$  quenches and large TF field, the rod's radial arm is short,  $\sim 3.5 \text{ cm}$ , and is welded into a solid 1.25 cm Inconel 625 plate resulting in a close box that significantly modifies the antenna spectrum. At the mid-plane major radius, the antenna limiters are 91.3 cm,  $\sim 0.8 \text{ cm}$  behind the main plasma limiters. The Faraday screen is at 91.7 cm and the straps are at 93.5 cm. The straps are separated by 25.75 cm on center and the straps are 10 cm wide.

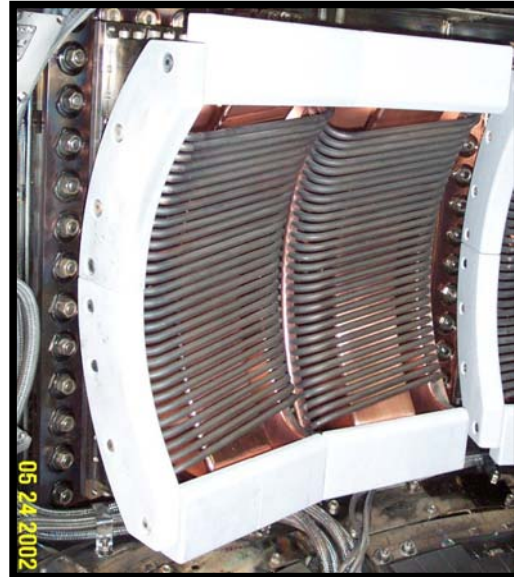


FIG. 1. Two strap antenna installed at D-port.



FIG. 2. Four strap fast wave antenna installed at J-port.

The J-port antenna (shown in FIG.2) is a folded strap design where the vacuum transmission line is parallel plate transmission line and the protection tiles are BN. The final parallel plate transmission line configuration was oriented such that over the majority of the path length the RF E-field is perpendicular to tokamak magnetic field. The Faraday screen is 50% optically transparent and parallel to the toroidal B-field. The rods have a “W” shape where the common leg bolted to the ground and the other two ends have a  $0.1 \Omega$  impedance to ground to minimize disruption induced currents. This  $0.1 \Omega$  connection consists of a nichrome wire coiled about an insulated bobbin with ceramic covering all but two nichrome tabs that make contact with the rod and antenna box. To eliminate arcing between this connection and the current strap, a stainless steel shield was installed to interrupt the arc path and shield the

ceramic from plasma. The rod's radial arm is  $\sim 10$  cm and the resulting antenna box is quite open. At the mid-plane major radius, the antenna limiters are 91.2 cm,  $\sim 0.7$  cm behind the main plasma limiters. The Faraday screen face is at 91.8 cm and the straps are at 93.6 cm. The current straps are separated by 18.6 cm on center and the straps are 8 cm wide.

In C-Mod, the antennas originally used molybdenum (Mo) protection tiles and the Mo core content was found to scale proportional to RF power.[5] Although the sources at the antenna are lower than the inner wall or divertor, the impurity screening at the outboard mid-plane is significantly poorer than the inner wall or divertor. One probable mechanism for the impurity production is the formation of rectified RF sheaths forming on metal surfaces. To eliminate the Mo source and prevent the sheaths from developing, the Mo tiles have been replaced with insulating BN, AXO5 grade from Carborundum. The BN significantly reduced the Mo antenna source rate simply by removing the Mo.

### 3.0 Antenna Performance

The J-port antenna performance is compared to the standard antennas in D and E-port. The plasma response to the application of E, J, and D-port antennas (0.8 MA, 5.2 T discharge) is shown in FIG. 3. The plasma transitions to H-mode with the application of 2 MW from D and E-port antennas. With application of J-port power, the stored energy, electron temperature, and neutron rate increase. The average density remains constant and the radiated power has a minor increase. This suggests the J-port power is coupled without significant impurity or density production. Furthermore, the present configuration has obtained a power density of  $\sim 11$  MW/m<sup>2</sup>.

A direct comparison of the heating efficiencies is shown in FIG.4. In an L-mode discharge, E, J, and D-port antennas injected 1.4 MW of RF into 0.8 MA, 5.2 T discharge. The plasma response was nearly identical suggesting the J-port antenna has a similar heating efficiency as D and E-port antennas. In a similar experiment, the power required to initiate a transition to H-mode was measured for each antenna to further investigate heating effectiveness. Within a single discharge, each antenna was pulsed for 0.2 sec and the H-mode power threshold measured. The three antennas measured nearly identical H-mode thresholds. A comparison of the loading shows that the J-port antenna loading is  $\sim 2.5$  times D and E-port antenna loading. For typical enhanced D $_{\alpha}$  H-mode discharges, the J-port loading is 45-54  $\Omega$ /m while D and E-port loading are 18-22  $\Omega$ /m. The similar heating efficiency suggests the higher loading is the result of better coupling.

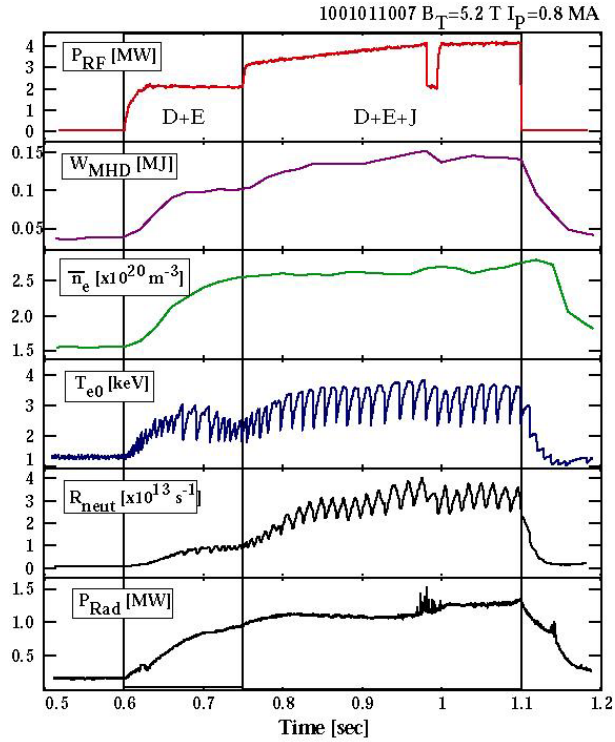


FIG. 3. Plasma response to RF power from the three antennas shows no degradation of H-mode performance with application of J-port antenna.

Although the heating efficiency is similar between the antennas, the voltage and power handling have been different. The D and E-port antennas have achieved maximum voltages of 40 kV in plasma operation. The J-port antenna has been modified in an iterative approach in order to achieve a maximum voltage of 35 kV. The D and E-port antennas have provided up to  $10 \text{ MW/m}^2$  without minimal impurity generation. The J-port design has been modified to obtain  $11 \text{ MW/m}^2$  previously limited either by arcing or impurity injections.

The arcing appeared to be related to where the RF E-field is parallel to the static B-field. Empirically the E-field (V/spacing) limit was determined to be  $\sim 15 \text{ kV/cm}$  for  $E\parallel B$ . This appears to agree with the voltage breakdown found by the JET RF group. [2] The breakdown voltage for  $E\perp B$  appears to be at least  $30 \text{ kV/cm}$ . The breakdown voltage in vacuum is greater than  $40 \text{ kV/cm}$ . This reduced breakdown voltage has been observed in the strip line power feeds and the antenna strap itself. The original and final transmission line configurations are shown in FIG. 5. In the region where the RF E-field is parallel to the static B-field, the voltage reaches a maximum value for  $78 \text{ MHz}$ . With this configuration, the maximum voltage during plasma operation was  $17 \text{ kV}$  corresponding to  $\sim 15 \text{ kV/cm}$ . Evidence of arcing was found in the transmission line during an inspection of the antenna. Upon orientating the RF E-field perpendicular to the static B-field, the antenna maximum voltage increased to  $25 \text{ kV}$  at  $78 \text{ MHz}$ . The arcing in this region has been eliminated up to voltages of  $35 \text{ kV}$  at  $70 \text{ MHz}$ . Further evidence of this empirical limit comes from the antenna strap itself. At  $78 \text{ MHz}$ , the maximum voltage was  $25 \text{ kV}$  but at  $70 \text{ MHz}$  the maximum voltage increased to  $30 \text{ kV}$ . This suggested the arcing location at the grounding bridge in the antenna strap itself, and a post campaign inspection found the arc damage at this location. At the bridge, the gap was increased and the electrode was shaped to reduce peaked fields resulting in  $35 \text{ kV}$  operations.

The reason for the degradation in breakdown voltage with  $E\parallel B$  can only be postulated. The estimated local E-fields are  $< 5 \text{ MV/m}$  and field emission becomes important near  $20 \text{ MV/m}$ . The electron mean free path is much greater than the electrode spacing indicating this combination of E-field, geometry and gas pressure is away from the minimum in the Paschen curve. Multipactoring also does not appear as a candidate. According to Craggs and Meeks [6], the ions govern the breakdown process since the electrons are swept from the spacing between the electrodes during a half cycle. Ion bombardment of the electrode and the corresponding secondary electron emission results in a streamer formation. The parallel B-field may enhance this process by preventing ion diffusion resulting in higher rectified fields.

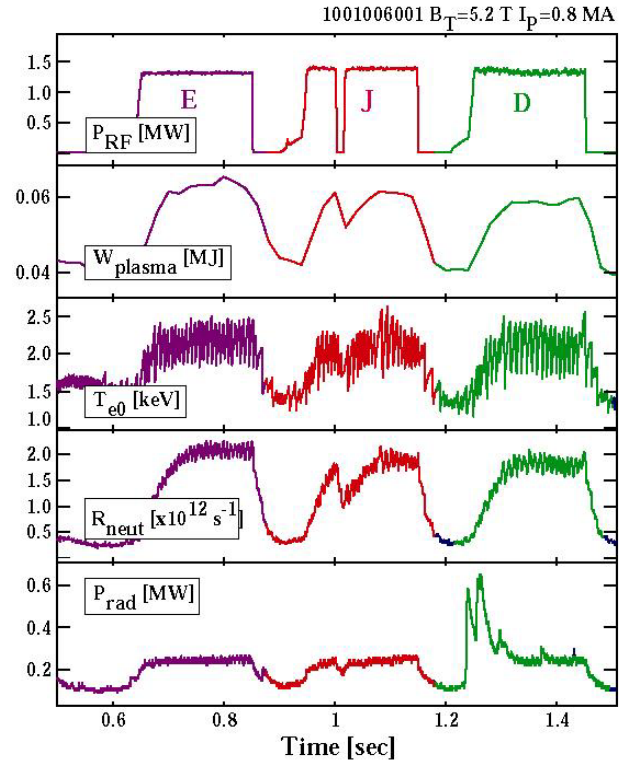


FIG. 4. In L-mode, the plasma response to RF power from the three antennas is nearly identical indicating the heating efficiency and impurity production is similar.



Impurity injections have been empirically determined to be from the metal protection tiles and exposed BN-metal interfaces. The J-port antenna has four separate back plate, antenna strap, and protection tile units (antenna units). These units were electrically connected via the back plates. Injections and hot spots were observed on the antenna using a visible camera. Melt damage was found on protection tiles that were on separate antenna units but not between tiles on the same unit. The injections were eliminated with the installation of a shorting strap along the front of the protection tiles. As mentioned above, BN was installed to reduce the metal impurities from the antennas. At BN-metal interfaces exposed to the plasma, injections were observed via visible camera, and melt damage was found at these interfaces. Field enhancement in the gap between the BN tile and metal surface has been postulated as the cause of the injections. With the BN-metal interfaces shielded from the plasma, the injections have been eliminated.

#### 4.0 Conclusion

A compact, 4-strap antenna has been developed and provides efficient plasma heating with power

density of  $11 \text{ MW/m}^2$ . This design utilizes a folded antenna strap and vacuum parallel plate transmission lines that are designed to have the RF E-field to be  $<15 \text{ kV/cm}$  in regions where  $E \parallel B$ . Furthermore, impurity generation and injections have been eliminated using BN protection tiles where the BN-metal interface is sufficiently shielded from the plasma.

This work is supported by Department of Energy Coop. Agreement DE-FC02-99ER54512.

- 
- [1] Y. Takase et al., "Design and analysis of the Alcator C-Mod two-strap ICRF antenna, 14<sup>th</sup> Symp. Fusion Engineering, San Diego (Piscataway, NJ):IEEE (1992), 118.
  - [2] A. Kaye et al., "Present and Future JET ICRF Antennae," Fusion Engineering and Design **24**, (1994) 1.
  - [3] A. Kaye, "ICRF system in the JET Pumped Divertor Configuration," 16<sup>th</sup> Symp. Fusion Engineering, Champaign (Piscataway, NJ):IEEE (1995), 736.
  - [4] G. Schilling et al., "Extension of Alcator C-Mod ICRF Experimental Capability," 13<sup>th</sup> Topical Conf. Radio Frequency Power in Plasmas, Annapolis (Melville, NY):AIP (1999), 429.
  - [5] B. Lipschultz et al., "A study of molybdenum influxes and transport in Alcator C-Mod," Nuclear Fusion **41**, (2001) 585.
  - [6] Craggs, "High-frequency breakdown of gases," in *Electrical Breakdown of Gases*, Meek and Craggs, Eds. New York: John Wiley & Sons, 1978, pp. 689-716.

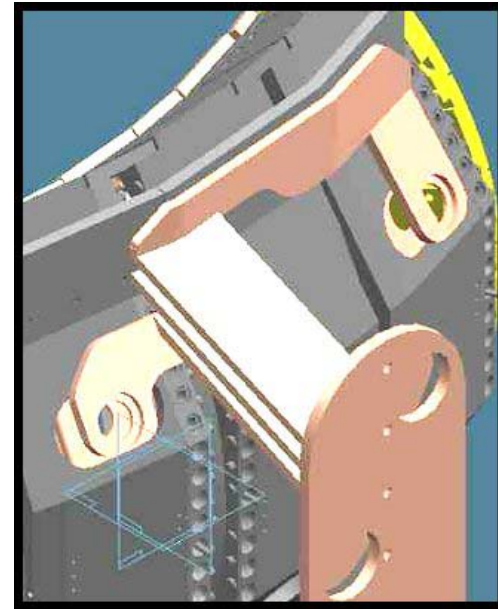
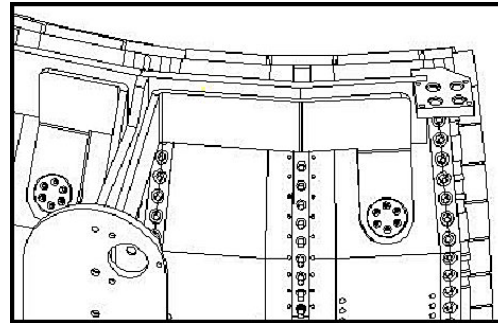


FIG. 5. Transmission line configuration for original design (a) has large region where  $E \parallel B$  and final configuration (b) where  $E \perp B$ .